

Metal–Metalloporphyrin Framework Modified with Flexible *tert*-Butyl Groups for Selective Gas Adsorption

Weijie Zhang,^[a, b] Lukasz Wojtas,^[a] Briana Aguila,^[a] Pingping Jiang,^{*,[b]} and Shengqian Ma^{*,[a]}

The rational design of multitopic organic linkers and access to the single-crystal structures of their metal–organic frameworks violate a long-standing thesis where it is expected to steer the system toward multifunctional MOFs. Here, a porphyrin that is covalently functionalized with pendant *tert*-butyl groups is used as a ligand having conformational freedom. The utilization of this custom-designed porphyrinic derivative in MOF synthesis yields a novel metal–metalloporphyrin framework (MMPF-14). As expected, the channels of MMPF-14, which are filled with flexible *tert*-butyl groups, act as molecular gates for the selective adsorption of gas molecules.

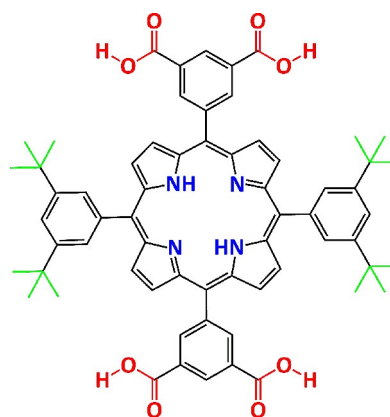
Over the past two decades metal–organic frameworks (MOFs)^[1] have been intensively developed as a promising class of functional porous materials. In particular, MOFs with specific composition and topology can be targeted by judicious selection of organic linkers and metal-based molecular building blocks (MBBs) that serve as nodes.^[2] These materials have received considerable attention due to the designability of their structures, tenability of pore sizes and modularity of properties, as well as great potential for applications in gas storage,^[3] gas separation,^[4] heterogeneous catalysis,^[5] sensors^[6] and other areas.^[7] In the reticular chemistry of MOFs where versatile custom-designed organic linkers are used, for example, metallosalen ligands^[8] and metalloporphyrin-based ligands,^[9] MOFs with a variety of functionalities can be expected.

Metal–metalloporphyrin frameworks (MMPFs), a subclass of MOFs recently demonstrated by our group^[10] and several other groups,^[11] have not only enriched the domain of porous materials, but have also been explored as promising candidates for the aforementioned applications. Although MMPF materials with various properties can be easily realized by modulating the metal sites and tailoring the coordination environments of

the metalloporphyrins, modification of MMPFs by the use of predesigned linkers has not been widely studied. One possible reason is that it is hard to achieve crystalline porous materials possessing the preferred interior decoration with organic functionalities. Therefore, the application of a modified porphyrin linker is much more desired.

It has been reported that the introduction of alkyl chains into MOFs could be used to tune the pore size which would result in better confinement of gas molecules in the pores.^[12] This prompted us to modify our established strategy based on the previously designed linker, 5,15-bis(3,5-dicarboxyphenyl)-10,20-bis(2,6-dibromophenyl)porphyrin (H_4dcbd).^[10a] Herein, we report an MMPF that is based upon a reported PtS topology net built from 4-connected building blocks of the 5,15-bis(3,5-dicarboxyphenyl)-10,20-bis(3,5-di-*tert*-butylphenyl)porphyrin (H_4dcdtp) linker (Scheme 1). Details on the chemical synthesis and characterization of the H_4dcdtp ligand are given in the Supporting Information.

Purple block crystals of $[Zn_8(\mu_2-HCO_2)](Zn-DCDTP)_4[EtOH][DMF]_2$, MMPF-14, were obtained by reacting $Zn(NO_3)_2 \cdot xH_2O$ with the H_4dcdtp ligand in *N,N*-dimethylformamide (DMF), ethanol, and HNO_3 (2 M) under solvothermal conditions for 72 h. Single-crystal X-ray diffraction analysis revealed that compound MMPF-14 crystallizes in the monoclinic space group $C2/c$. As expected, not all atoms of the flexible *tert*-butyl substituents can be located in the single-crystal structure refinement due to the high disorder. Zinc(II) in the porphyrin core is located in close to perfect square-planar $\{N_4\}$ geometry, coordinated to four nitrogen atoms (four porphyrinic nitrogens). The Zn–N bond lengths range from 2.027 Å to 2.040 Å. In MMPF-14, the inorganic building unit is the $Zn_2(\mu_2-HCO_2)(COO)_4$ dimer MBB



Scheme 1. 5,15-Bis(3,5-dicarboxyphenyl)-10,20-bis(3,5-di-*tert*-butylphenyl)porphyrin (H_4dcdtp): the custom-designed ligand that serves as a linker in MMPF-14.

[a] W. Zhang, L. Wojtas, B. Aguila, Prof. S. Ma
Department of Chemistry
University of South Florida
4202 East Fowler Avenue Tampa, FL 33620 (USA)
E-mail: sqma@usf.edu

[b] W. Zhang, Prof. P. Jiang
The Key Laboratory of Food Colloids and Biotechnology
Ministry of Education
School of Chemical and Material Engineering
Jiangnan University, Wuxi 214122 (P. R. China)
E-mail: ppjiang@jiangnan.edu.cn

Supporting information and the ORCID identification number(s) for the author(s) of this article can be found under <http://dx.doi.org/10.1002/cplu.201600158>.



This article is part of a Special Issue on "Coordination Polymers/MOFs". To view the complete issue, visit: <http://dx.doi.org/10.1002/cplu.v81.8>.

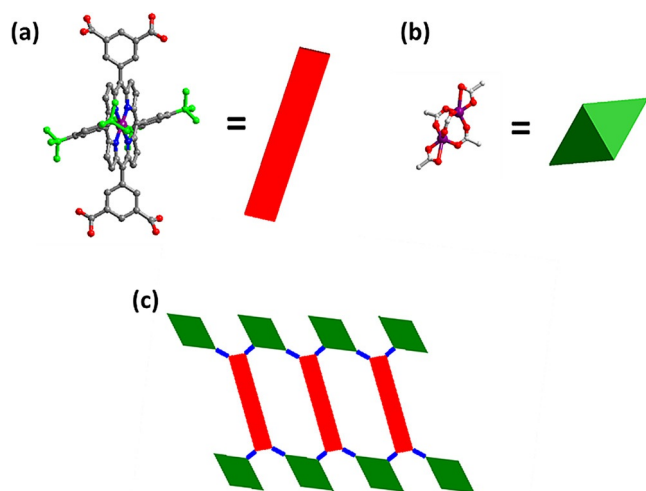


Figure 1. From the crystal structure of $[\text{Zn}_6(\mu_2\text{-HCO}_2)](\text{Zn-DCDTP})_4[\text{EtOH}][\text{DMF}]_2$ (MMPF-14): a) H_4dcdtp (red rectangle) and b) $\text{Zn}_2(\mu_2\text{-HCO}_2)(\text{COO})_4$ (green rhombus or diamond) building units form a **PtS** net c) in the periodic crystal structure. Hydrogen atoms, guest molecules, and HCO_2^{2-} ions on MMBs have been omitted for clarity. Zn purple, C in porphyrin ligand gray, C in *tert*-butyl groups green, O red, N blue.

that is linked by carboxylate oxygens and HCO_2^{2-} ions arising from DMF (Figure 1 b). To be more specific, Zn is five-coordinate with five oxygen atoms from one monodentate chelating $\mu_1\text{-}\eta_2$ carboxylate, two bidentate bridging $\mu_2\text{-}\eta_1\eta_1$ carboxylates, and HCO_2^{2-} ions. The other Zn ion is also five-coordinate and has the same coordination environment. The two pentacoordinate Zn atoms are linked by two $\mu_2\text{-}\eta_1\eta_1$ carboxylate groups and HCO_2^{2-} ions to form a dimer. Considering the points-of-extension of the carboxylate C atoms of MBBs and four carbon atoms of the organic unit, they can be simplified as a rhombus and a rectangle as shown in Figure 1 a,b, respectively. In the overall crystal structures, the rhombus and rectangle units are linked to produce a 3D periodic structure (Figure 1 c). Overall, the asymmetric unit of MMPF-14 consists of a dimeric Zn cluster and a metallic dcdtp ligand, which gives rise to the well-known 4,4-connected **PtS** network with the point symbol $\{4^2.8^4\}$.^[13]

Obviously, the flexible *tert*-butyl units of the H_4dcdtp linkers point into the channels along the *c* axis, forming a molecular gate for gas separation and adsorption (Figure 2). The size of the pores in MMPF-14 is about 3.7 Å. The dihedral angles between the phenyl rings bearing the carboxylates in the porphyrin ligand and the porphyrin plane are 72.34° and 76.81°, respectively. Notably, for the other two phenyl rings, the angle value decreases to 55.83° and 57.60°, which is much lower than some existing data.^[10,11] Due to the steric repulsion induced by 3,5-disubstitution, coplanarity of the phenyl ring with the porphyrin plane caused by conjugation is no longer preferred. This strongly indicates that the conformational freedom in H_4dcdtp is much greater than that in a conventional porphyrin ligand. In addition, the solvent-accessible volume in MMPF-14 is 47.6% calculated using the PLATON routine.^[14] This provides sufficient space for solvent molecules and charge-balancing counterions for the framework.

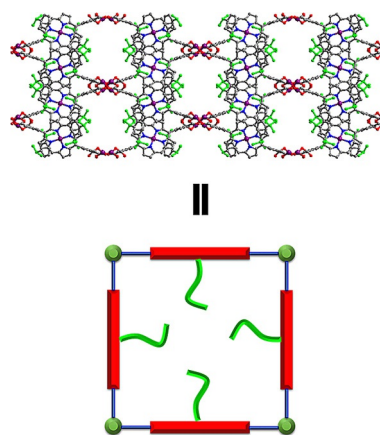


Figure 2. View of the 3D structure of MMPF-14 along the *c*-axis. Zn purple, C in porphyrin ligand gray, C in *tert*-butyl groups green, O red, N blue; H atoms are omitted for clarity.

Thermogravimetric analysis (TGA) of MMPF-14 reveals a moderate 13% weight loss within the temperature range of 50–360 °C, corresponding to the loss of H_2O , ethanol, and DMF molecules (Figure 3 a). A sharp weight-loss step of over 47% was observed as the temperature increased from 360 to 700 °C, indicating the structural decomposition of MMPF-14. Additionally, TGA traces for MMPF-14 crystals after activation with supercritical CO_2 fluid do not show significant weight loss up to 360 °C, and the PXRD patterns of MMPF-14 after activation is also similar to the simulated pattern, indicating that the pores are fully evacuated while the framework integrity remains and is thermally stable (Figures S3 and S4). The purity of bulk samples of MMPF-14 is confirmed by the agreement of the experimental and calculated powder X-ray diffraction (PXRD) patterns.

N_2 adsorption isotherms of MMPF-14 were collected at 77 K, and a very limited amount of N_2 ($28 \text{ cm}^3 \text{ g}^{-1}$) can be adsorbed as shown in Figure 4 a. In contrast, greater H_2 uptake ($85 \text{ cm}^3 \text{ g}^{-1}$) is observed and substantial O_2 uptake of $107 \text{ cm}^3 \text{ g}^{-1}$ is also found at the saturation pressure of 150 Torr at 77 K. At 273 K and 1 atmosphere pressure, MMPF-14 can adsorb $54 \text{ cm}^3 \text{ g}^{-1}$ CO_2 (Figure 4 b), whereas its uptake capacity for CH_4 (ca. $7 \text{ cm}^3 \text{ g}^{-1}$) and N_2 (ca. $2 \text{ cm}^3 \text{ g}^{-1}$) is very low. In order to confirm that CO_2 is adsorbed within the intralattice voids of the MOF rather than on the surface of the solid, the gas sorption of MMPF-14 for CO_2 at 195 K was examined; CO_2 adsorption on this MOF increased at a relatively low pressure (Figure S5). The interesting selective adsorption of H_2 and O_2 over N_2 , as well as CO_2 over CH_4 and N_2 observed for MMPF-14 can be presumably attributed to the effect of the *tert*-butyl groups in the channels. These serve as gates^[4d] to exclude the larger molecules of N_2 and CH_4 with kinetic diameters of 3.64 and 3.8 Å, respectively, and allow the entry of the smaller molecules H_2 (kinetic diameter 2.89 Å), O_2 (kinetic diameter 3.46 Å), and CO_2 (kinetic diameter 3.3 Å).^[4c] We also estimate the isosteric heats of adsorption (Q_{st}) for CO_2 based upon the Clausius–Clapeyron equation by differentiation of the dual-Langmuir–Freundlich fits of the isotherms at temperatures of 273 and 298 K with temperature-dependent parameters.^[15] As shown in

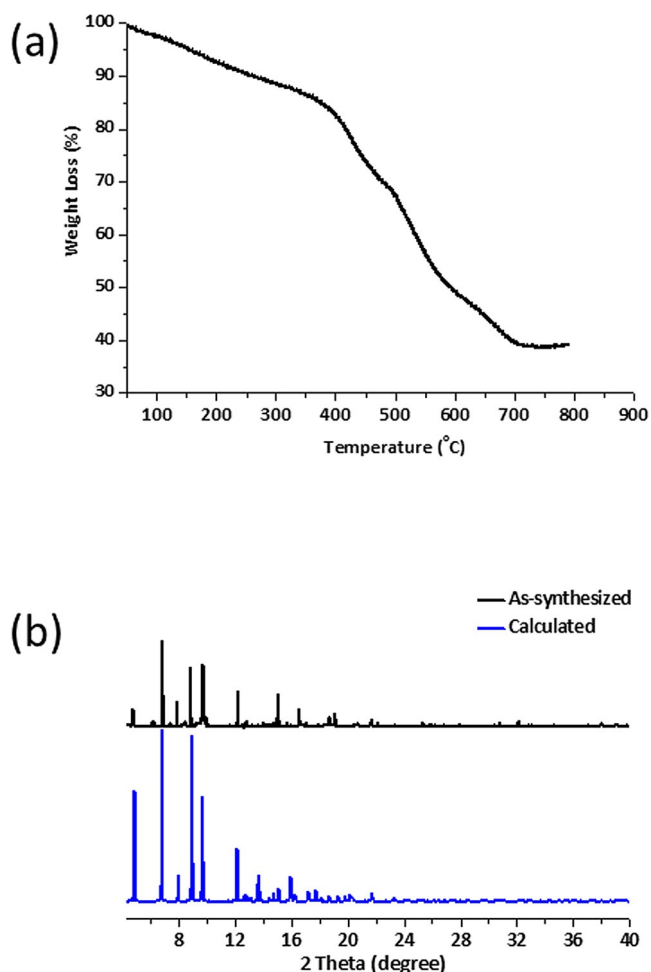


Figure 3. a) TG profile of MMPF-14 before activation, b) PXRD patterns for as-synthesized MMPF-14 and calculated pattern.

Figure S7, at close to zero loading, for CO₂ in MMPF-14 $Q_{st} \approx 34 \text{ kJ mol}^{-1}$, which is comparable to the highest of the reported porphyrin-based MOFs.^[10c,d,f] We tentatively attribute the relatively high Q_{st} value to the modified *tert*-butyl groups, since pendant *tert*-butyl groups can boost the interactions with CO₂ molecules more in a porous framework.^[12]

In summary, a rare example of Zn-based porous metal metalloporphyrin-organic framework with PtS topology, MMPF-14, has been constructed based upon a custom-designed porphyrin ligand featuring pendant *tert*-butyl groups. MMPF-14 exhibits permanent porosity and demonstrates interesting selective gas adsorption behavior. Ongoing work in our laboratories includes designing new variants of porphyrin-based ligands for the construction of functional MMPF materials and exploring their applications in sensor, catalysis and photoreaction systems.

Experimental Section

Purple block crystals of MMPF-14, $[\text{Zn}_6(\mu_2\text{-HCO}_2)](\text{Zn-DCDTP})_4[\text{EtOH}][\text{DMF}]_2$ were prepared by reacting $\text{Zn}(\text{NO}_3)_2 \cdot x\text{H}_2\text{O}$ with H_4dcdtp in *N,N*-dimethylformamide (0.8 mL of DMF, 0.2 mL of ethanol, and 50 μL 2 M HNO_3) under solvothermal conditions for

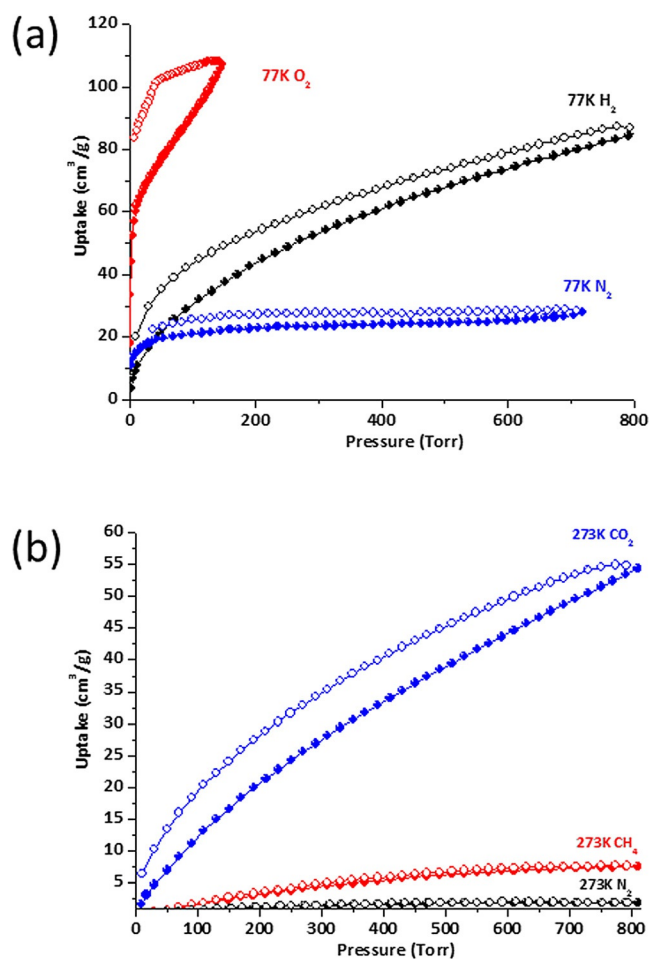


Figure 4. a) Gas adsorption isotherms of MMPF-14 at a) 77 K and b) 273 K.

72 h. Crystal details, PXRD, TG analysis, gas sorption, and catalytic details are provided supplied in the Supporting Information. CCDC 1408968 contains the supplementary crystallographic data for this paper. These data can be obtained free of charge from The Cambridge Crystallographic Data Centre.

Acknowledgements

We thank the NSF (DMR-1352065) and the USF for financial support of this work. W.Z. acknowledges support from the China Scholarship Council (CSC).

Keywords: metal-organic frameworks • porphyrins • selective gas adsorption

- [1] a) H. C. Zhou, J. R. Long, O. M. Yaghi, *Chem. Rev.* **2012**, *112*, 673–674; b) H. C. Zhou, S. Kitagawa, *Chem. Soc. Rev.* **2014**, *43*, 5415–5418; c) B. Li, M. Chrzanowski, Y. Zhang, S. Ma, *Coord. Chem. Rev.* **2016**, *307*, 106.
[2] a) O. M. Yaghi, G. Li, H. Li, *Nature* **1995**, *378*, 703–706; b) J. T. Jones, T. Hasell, X. Wu, J. Bacsá, K. E. Jelfs, M. Schmidtman, S. Y. Chong, D. J. Adams, A. Trewin, F. Schiffman, F. Cora, B. Slater, A. Steiner, G. M. Day, A. I. Cooper, *Nature* **2011**, *474*, 367–371; c) M. Eddaoudi, D. B. Moler, H. Li, B. Chen, T. M. Reineke, M. O’Keeffe, O. M. Yaghi, *Acc. Chem. Res.* **2001**, *34*, 319–330; d) Y. He, B. Li, M. O’Keeffe, B. Chen, *Chem. Soc. Rev.* **2014**, *43*, 5618–5656; e) N. Stock, S. Biswas, *Chem. Rev.* **2012**, *112*, 933–969; f) W.-Y. Gao, S. Ma, *Comments Inorg. Chem.* **2014**, *34*, 125.

- [3] a) L. J. Murray, M. Dinca, J. R. Long, *Chem. Soc. Rev.* **2009**, *38*, 1294–1314; b) S. Ma, H.-C. Zhou, *Chem. Commun.* **2010**, *46*, 44–53; c) M. P. Suh, H. J. Park, T. K. Prasad, D.-W. Lim, *Chem. Rev.* **2012**, *112*, 782–835; d) H. Wu, Q. Gong, D. H. Olson, J. Li, *Chem. Rev.* **2012**, *112*, 836–868; e) R. B. Getman, Y. S. Bae, C. E. Wilmer, R. Q. Snurr, *Chem. Rev.* **2012**, *112*, 703–723.
- [4] a) J. R. Li, J. Sculley, H. C. Zhou, *Chem. Rev.* **2012**, *112*, 869–932; b) S. Ma, *Pure Appl. Chem.* **2009**, *81*, 2235–2251; c) J.-R. Li, R. J. Kuppler, H. C. Zhou, *Chem. Soc. Rev.* **2009**, *38*, 1477–1504; d) S. Ma, D. Sun, X.-S. Wang, H.-C. Zhou, *Angew. Chem. Int. Ed.* **2007**, *46*, 2458; *Angew. Chem.* **2007**, *119*, 2510.
- [5] a) J. Lee, O. K. Farha, J. Roberts, K. A. Scheidt, S. T. Nguyen, J. T. Hupp, *Chem. Soc. Rev.* **2009**, *38*, 1450–1459; b) A. Corma, H. Garcia, F. X. Llabres i Xamena, *Chem. Rev.* **2010**, *110*, 4606–4655; c) M. Yoon, R. Srirambalaji, K. Kim, *Chem. Rev.* **2012**, *112*, 1196–1231; d) B. Li, K. Leng, Y. Zhang, J. Dynes, J. Wang, Y. Hu, D. Ma, Z. Shi, L. Zhu, D. Zhang, Y. Sun, M. Chrzanowski, S. Ma, *J. Am. Chem. Soc.* **2015**, *137*, 4243–4248; e) W.-Y. Gao, H. Wu, K. Leng, Y. Sun, S. Ma, *Angew. Chem. Int. Ed.* **2016**, *55*, 5472–5476; *Angew. Chem.* **2016**, *128*, 3290–3290.
- [6] a) B. Chen, S. Xiang, G. Qian, *Acc. Chem. Res.* **2010**, *43*, 1115–1124; b) L. E. Kreno, K. Leong, O. K. Farha, M. Allendorf, R. P. Van Duyne, J. T. Hupp, *Chem. Rev.* **2012**, *112*, 1105–1125; c) Y. Cui, Y. Yue, G. Qian, B. Chen, *Chem. Rev.* **2012**, *112*, 1126–1162; d) Y.-H. Shih, C.-P. Fu, W.-L. Liu, C.-H. Lin, H.-Y. Huang, S. Ma, *Small* **2016**, *12*, 2057–2066.
- [7] a) C. Wang, T. Zhang, W. Lin, *Chem. Rev.* **2012**, *112*, 1084–1104; b) H. Zhao, Z. R. Qu, H. Y. Ye, R. G. Xiong, *Chem. Soc. Rev.* **2008**, *37*, 84–100; c) S. Shaik, S. Cohen, Y. Wang, H. Chen, D. Kumar, W. Thiel, *Chem. Rev.* **2010**, *110*, 949–1017; d) P. Horcajada, R. Gref, T. Baati, P. K. Allan, G. Maurin, P. Couvreur, G. Férey, R. E. Morris, C. Serre, *Chem. Rev.* **2012**, *112*, 1232–1268; e) A. Bétard, R. A. Fischer, *Chem. Rev.* **2012**, *112*, 1055–1083; f) Y. Chen, V. Lykourinou, C. Vetromile, T. Hoang, L. J. Ming, R. W. Larsen, S. Ma, *J. Am. Chem. Soc.* **2012**, *134*, 13188–13191.
- [8] a) C. Zhu, G. Yuan, X. Chen, Z. Yang, Y. Cui, *J. Am. Chem. Soc.* **2012**, *134*, 8058–8061; b) J. M. Falkowski, C. Wang, S. Liu, W. Lin, *Angew. Chem. Int. Ed.* **2011**, *50*, 8674–8678; *Angew. Chem.* **2011**, *123*, 8833–8837; c) A. M. Shultz, A. A. Sarjeant, O. K. Farha, J. T. Hupp, S. T. Nguyen, *J. Am. Chem. Soc.* **2011**, *133*, 13252–13255; d) F. Song, C. Wang, J. M. Falkowski, L. Ma, W. Lin, *J. Am. Chem. Soc.* **2010**, *132*, 15390–15398.
- [9] W. Y. Gao, M. Chrzanowski, S. Ma, *Chem. Soc. Rev.* **2014**, *43*, 5841–5866.
- [10] a) L. Meng, Q. Cheng, C. Kim, W. Y. Gao, L. Wojtas, Y. S. Chen, M. J. Zaworotko, X. P. Zhang, S. Ma, *Angew. Chem. Int. Ed.* **2012**, *51*, 10082–10085; *Angew. Chem.* **2012**, *124*, 10229–10232; b) W. Y. Gao, L. Wojtas, S. Ma, *Chem. Commun.* **2014**, *50*, 5316–5318; c) X. S. Wang, M. Chrzanowski, C. Kim, W. Y. Gao, L. Wojtas, Y. S. Chen, X. Peter Zhang, S. Ma, *Chem. Commun.* **2012**, *48*, 7173–7175; d) X.-S. Wang, M. Chrzanowski, W.-Y. Gao, L. Wojtas, Y.-S. Chen, M. J. Zaworotko, S. Ma, *Chem. Sci.* **2012**, *3*, 2823–2827; e) X. S. Wang, M. Chrzanowski, L. Wojtas, Y. S. Chen, S. Ma, *Chem. Eur. J.* **2013**, *19*, 3297–3301; f) W.-Y. Gao, Z. Zhang, L. Cash, L. Wojtas, Y.-S. Chen, S. Ma, *CrystEngComm* **2013**, *15*, 9320–9323; g) Y. Chen, T. Hoang, S. Ma, *Inorg. Chem.* **2012**, *51*, 12600–12602; h) X. S. Wang, L. Meng, Q. Cheng, C. Kim, L. Wojtas, M. Chrzanowski, Y. S. Chen, X. P. Zhang, S. Ma, *J. Am. Chem. Soc.* **2011**, *133*, 16322–16325; i) W. Zhang, W.-Y. Gao, T. Pham, P. Jiang, S. Ma, *Cryst. Growth Des.* **2016**, *16*, 1005.
- [11] a) M. Zhao, S. Ou, C. D. Wu, *Acc. Chem. Res.* **2014**, *47*, 1199–1207; b) D. Feng, Z.-Y. Gu, Y.-P. Chen, J. Park, Z. Wei, Y. Sun, M. Bosch, S. Yuan, H.-C. Zhou, *J. Am. Chem. Soc.* **2014**, *136*, 17714–17717; c) J. A. Johnson, X. Zhang, T. C. Reeson, Y. S. Chen, J. Zhang, *J. Am. Chem. Soc.* **2014**, *136*, 15881–15884; d) H. L. Jiang, D. Feng, K. Wang, Z. Y. Gu, Z. Wei, Y. P. Chen, H. C. Zhou, *J. Am. Chem. Soc.* **2013**, *135*, 13934–13938; e) D. Feng, Z. Y. Gu, J. R. Li, H. L. Jiang, Z. Wei, H. C. Zhou, *Angew. Chem. Int. Ed.* **2012**, *51*, 10307–10310; *Angew. Chem.* **2012**, *124*, 10453–10456; f) A. Fateeva, P. A. Chater, C. P. Ireland, A. A. Tahir, Y. Z. Khimiyak, P. V. Wiper, J. R. Darwent, M. J. Rosseinsky, *Angew. Chem. Int. Ed.* **2012**, *51*, 7440–7444; *Angew. Chem.* **2012**, *124*, 7558–7562; g) T. F. Liu, D. Feng, Y. P. Chen, L. Zou, M. Bosch, S. Yuan, Z. Wei, S. Fordham, K. Wang, H. C. Zhou, *J. Am. Chem. Soc.* **2015**, *137*, 413–419; h) X. L. Yang, M. H. Xie, C. Zou, Y. He, B. Chen, M. O’Keeffe, C. D. Wu, *J. Am. Chem. Soc.* **2012**, *134*, 10638–10645; i) C. Zou, Z. Zhang, X. Xu, Q. Gong, J. Li, C. D. Wu, *J. Am. Chem. Soc.* **2012**, *134*, 87–90; j) M. E. Kosal, J. H. Chou, S. R. Wilson, K. S. Suslick, *Nat. Mater.* **2002**, *1*, 118–121; k) E. A. Dolgoplova, D. E. Williams, A. B. Greytak, A. M. Rice, M. D. Smith, J. A. Krause, N. B. Shustova, *Angew. Chem. Int. Ed.* **2015**, *54*, 13639–13643; *Angew. Chem.* **2015**, *127*, 13843–13847; l) D. E. Williams, J. A. Rietman, J. M. Maier, R. Tan, A. B. Greytak, M. D. Smith, J. A. Krause, N. B. Shustova, *J. Am. Chem. Soc.* **2014**, *136*, 11886–11889; m) K. Lu, C. He, W. Lin, *J. Am. Chem. Soc.* **2014**, *136*, 16712–16715; n) G. Nandi, I. Goldberg, *Chem. Commun.* **2014**, *50*, 13612–13615.
- [12] a) L. Liu, S. G. Telfer, *J. Am. Chem. Soc.* **2015**, *137*, 3901–3909; b) S. Henke, R. A. Fischer, *J. Am. Chem. Soc.* **2011**, *133*, 2064–2067; c) Z. Zhang, H. T. Nguyen, S. A. Miller, S. M. Cohen, *Angew. Chem. Int. Ed.* **2015**, *54*, 6152–6157; *Angew. Chem.* **2015**, *127*, 6250–6255; d) A. Schneemann, E. D. Bloch, S. Henke, P. L. Llewellyn, J. R. Long, R. A. Fischer, *Chem. Eur. J.* **2015**, *21*, 18764–18769; e) S. C. Xiang, Z. Zhang, C. G. Zhao, K. Hong, X. Zhao, D. R. Ding, M. H. Xie, C. D. Wu, M. C. Das, R. Gill, K. M. Thomas, B. Chen, *Nat. Commun.* **2011**, *2*, 204; f) M. C. Das, Q. Guo, Y. He, J. Kim, C. G. Zhao, K. Hong, S. Xiang, Z. Zhang, K. M. Thomas, R. Krishna, B. Chen, *J. Am. Chem. Soc.* **2012**, *134*, 8703–8710.
- [13] a) M. O’Keeffe, O. M. Yaghi, *Chem. Rev.* **2012**, *112*, 675–702; b) B. Chen, N. W. Ockwig, F. R. Fronczek, D. S. Contreras, O. M. Yaghi, *Inorg. Chem.* **2005**, *44*, 181–183.
- [14] A. L. Spek, *J. Appl. Crystallogr.* **2003**, *36*, 7–13.
- [15] a) R. Krishna, *Microporous Mesoporous Mater.* **2014**, *185*, 30–50; b) Y. He, R. Krishna, B. Chen, *Energy Environ. Sci.* **2012**, *5*, 9107–9120.

Manuscript received: March 31, 2016

Accepted Article published: April 29, 2016

Final Article published: May 17, 2016